



SPACE RIDER: Mission Analysis and Flight Mechanics of the Future European Reusable Space Transportation System

D. Bonetti¹, G. De Zaiacomo¹, G. Blanco Arnao¹, G. Medici¹

Abstract

This paper presents the Space Rider Mission Analysis activities carried out during the phase A/B1 of the Space Rider ESA program. The Space Rider program is an ESA development program that aims to provide Europe with an affordable, independent, reusable end-to-end integrated space transportation system for routine access and return from low orbit. It will be used to transport payloads for an array of applications, orbit altitudes and inclinations. This paper presents the Mission Engineering process, which includes a range of activities in support to the system design: assessment of the orbital scenarios and definition of the re-entry opportunities to target the desired landing sites, computation of the End-to-End (de-orbiting to touchdown) optimum reference trajectories, sizing trajectories for subsystems specifications, characterization of the Entry Corridor for trajectory design (focusing in particular on the supersonic and transonic phases not covered by the IXV), specification of the optimum Centre of Gravity (CoG) box compatible with layout capabilities, selection of the optimum Angle of Attack (AoA) trim line to be flown and Flying Qualities performance, assessment of the mission performance through Monte Carlo simulation campaigns, analysis of the visibility from ground stations and support to safety analyses (off-nominal footprints).

Keywords: *Mission Analysis, Flying Qualities, End-to-End, Space Rider*

1. Introduction

On February, 11th, 2015, the successful flight of the Intermediate eXperimental Vehicle (IXV) allowed demonstrating the European independent capability to return from space. IXV (Fig 2) was a lifting body vehicle with two movable flaps for aerodynamic control that performed a suborbital mission, allowing in-flight demonstration of critical technologies for hypersonic flight conditions and successive re-entry from LEO. After being injected by VEGA in a 400km altitude orbit, IXV performed a successful entry targeting the desired parachutes triggering conditions, to start the final descent for a safe splashdown in the Pacific Ocean.

Leveraging on IXV development, qualification and mission success, intended as an European “intermediate” step toward multiple future space applications, the European Space Agency (ESA) initiated an effort to develop a sustainable reusable European space transportation system integrated with the VEGA C launcher, the Space Rider (SR) currently under development, to enable routine launch and return space missions [1]. VEGA C and the Space Rider constitute an Integrated Space Transportation System (ISTS, Fig 1), composed by:

- Module 1 = the Launch and AVUM Orbital Module (AOM), physically consisting of the Vega C launcher with a specifically adapted AVUM, with the latter acting as orbital service module up to de-orbit boost and separation from the Re-entry Module (RM).
- Module 2 = the Re-entry Module (RM), starting its active role at orbit acquisition, performing the in-orbit payload operations with the AOM support, and remaining active until completion of landing on ground.

The Space Rider RM will have a Multi-Purpose Cargo Bay (MPCB) able to integrate a number of modular payloads to fulfill multiple mission objectives and to perform experimentation of payloads for multiple space applications.

¹DEIMOS Space S.L.U., Ronda de Poniente 19, Tres Cantos, 28760, Spain, davide.bonetti@deimos-space.com



Fig 1. The Space Rider concept
(Credits: ESA)



Fig 2. The IXV after the successful re-entry (Credits: ESA)

Designed to be an operational demonstrator able to perform at least 5 missions, the Space Rider will have to support orbital operations in multiple orbital scenarios, from SSO to equatorial, deorbit and flight back to Earth with high maneuverability and controllability throughout all flight regimes (i.e. hypersonic, supersonic, transonic, subsonic) to perform a safe and precise soft-landing on ground under parafoil. The vehicle is therefore required to have the flexibility to ensure that environmental and operational unexpected events are mitigated and to guarantee the accomplishment of the mission objectives in compliance to stringent safety constraints in case of failure.

While the heritage from the IXV mission is highly applicable to the mission design for SR, IXV was injected directly by VEGA in a suborbital trajectory, and did not perform an orbital phase nor needed to carry out a deorbit maneuver. Also, IXV used a supersonic drogue chute, and hence it did not fly through the transonic regime. Moreover, the SR is an operational vehicle, that will support a range of mission types. Hence SR presents new challenges for the mission design of the coasting and re-entry phase and requires the development of European capabilities to fly the lifting vehicle aeroshape through the transonic regime to a subsonic drogue chute, which places in particular constraints and challenges on the vehicle's flying qualities during the lower Mach regime from Mach 1.2 to Mach 0.7.

DEIMOS Space is in charge of the Mission Engineering activities, currently at the System PDR, including end-to-end Mission Analysis and Flying Qualities, for the Space Rider, a role that also had in the successful IXV, from the design phase up to launch and flight operations [2].

This paper presents the Mission Engineering activities of the Space Rider vehicle carried out in the phase A/B1 of the programme in support to the system design. The assessment of the orbital scenarios and the definition of the re-entry opportunities were performed, to target the desired landing site within the proposed landing site network. The specification of the optimum Centre of Gravity (CoG) box compatible with the layout capabilities was carried out, in addition to the characterization of the Entry Corridor for trajectory design (focusing in particular on the supersonic and transonic phases not covered by the IXV), the selection of the optimum Angle of Attack (AoA) trim line to be flown, and the associated Flying Qualities performance. End-to-end (de-orbiting to touchdown) optimum reference trajectories were computed, as well as sizing trajectories for subsystems specifications (e.g. TPS, parachutes), and the mission performance were assessed through Monte Carlo simulation campaigns. Finally, the analysis of the visibility of the SR from ground stations during the flight was carried out, and support to safety analyses (off-nominal footprints) was provided.

2. Space Rider Mission and Vehicle Overview

At the beginning of the SR programme, a trade off was carried out to at first select the most appropriate aeroshape class among different classes, and then define the baseline configuration within the selected class (see [3] and section 3). The current baseline design of the Space Rider Re-entry Module has the same aeroshape and size as the IXV (shown in Fig 4). The SR RM is a lifting body, having no wings, and provides a lift-to-drag ratio of about 0.7 in the hypersonic regime.

With respect to the IXV mission, the SR mission will have to support orbital operations in multiple orbital scenarios, deorbit and re-entry to perform a safe and precise soft-landing on ground under parafoil (Fig 3). In particular:

- The SR ISTS is launched from Kourou onboard the Vega C launcher and injected into orbit.
- During the orbital phase the SR objective is to accomplish the goals for the specific orbital mission. Target orbits currently considered are circular, have an altitude of 400:500 km, and with an inclination range from equatorial to SSO, depending on the mission objectives.
- At deorbiting, the SR executes a deorbit boost to target the desired conditions at the EIP. After the deorbit maneuver is completed the RM separates from the AOM and performs a ballistic coasting phase prior to entry. Attitude control during this orbital phase is carried out by means of the Reaction Control System (RCS). The targeted conditions at the EIP are typical of LEO return missions, with co-rotating velocities beyond 7.4 km/s.
- The RM then performs a guided gliding re-entry from the EIP until low supersonic regime (at Mach 1.6), when transition into TAEM phase occurs. The TAEM phase objective is to get the vehicle to the desired conditions (position, velocity, attitude) at the DRS triggering.
- At approximately Mach 0.8 the DRS sequence (this terminology was inherited by IXV) is triggered, and a pilot chute, a conical ribbon drogue, and a Disk-Gap-Band drogue are deployed successively to slow the vehicle down toward the desired conditions for the parafoil deployment, that occurs at 6 km of altitude and about Mach 0.12. The parafoil allows to glide with a shallow flight path angle and to maneuver to reach the desired landing site.
- The flight terminates with an approach and landing phase at the desired landing site. In this phase the vehicle performs a flare maneuver to achieve the proper touchdown conditions.

Multiple orbital mission scenarios have been considered, according to the system needs and specifications provided. The process has been highly dynamic with the main objective of contributing to the feasibility verification of the mission scenarios under investigation from the mission analysis standpoint and in particular from the fuel consumptions point of view. Contributions from the GNC subsystem have been integrated in the total fuel consumptions budget estimations.

Depending on the orbital scenario and on the payload, different landing sites are considered, and different vehicle configurations are possible (see section 3). Therefore, the Entry and TAEM phases could vary accordingly. In particular, considering that the entry mission design strategy is to target the same FPA at the EIP as IXV (see section 0), the re-entry phase will depend on the co-rotating velocity at the EIP, the RM mass, and the targeted downrange to be flown during entry.

The current *baseline mission* includes a return from a medium inclination orbit (37 deg), with the RM in the maximum mass configuration (2549 kg), and landing at Santa Maria, Azores, while the *backup mission* considers a return from a quasi-equatorial orbit (5.3 deg) and landing at Kourou.

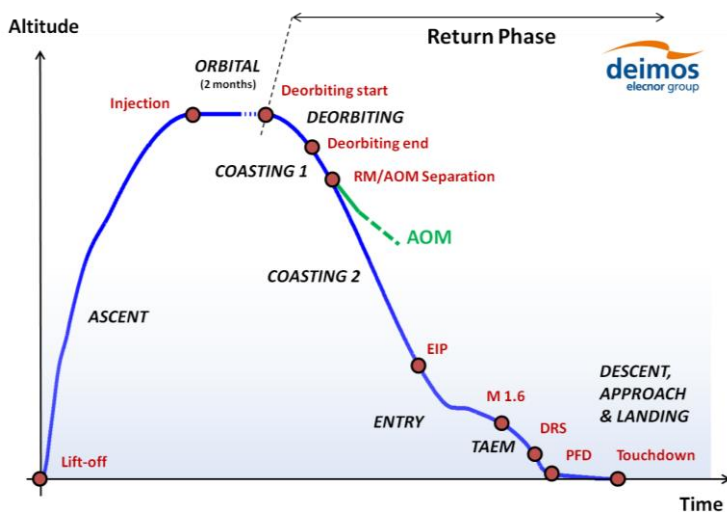


Fig 3. The Space Rider reference mission

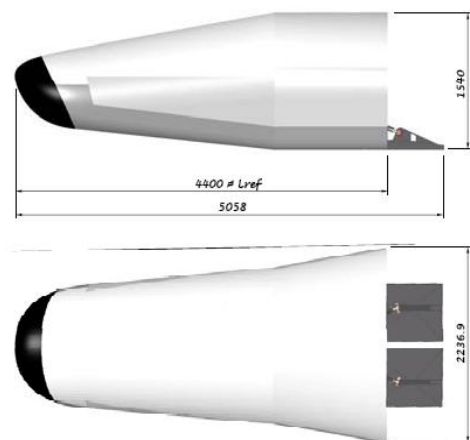


Fig 4. The IXV/SR RM aeroshape (Credits: TAS)

3. Vehicle Configuration Design

In a re-entry vehicle the AoA profile is strongly linked with the mission feasibility and hence its selection and assessment is strictly coupled with the trajectory design. The optimum AoA profile is obtained from an end to end analysis of the vehicle flying qualities and flight mechanics performance in the full range of flight regimes covered by the mission: from rarefied flow, through hypersonic, supersonic and down to subsonic.

The AoA profile (trim line) is the result of a trim process (null moments) where, for a given aerodynamic shape, the vehicle Centre of Gravity (CoG) location play a key role in combination with the aerodynamic surface deflections. Basically, for a given CoG location, an AoA-Mach corridor can be obtained: in this way it is possible to map the feasible CoG locations that are compatible with the applicable constraints and under within the applicable dispersions. In the IXV mission engineering [2], an overall design process was implemented where key vehicle parameters (CoG, AoA profile, Elevators deflections) were coupled through flying qualities (trim, stability and controllability aspects) and detailed mission analysis performance (thermo mechanical loads, landing accuracy, visibility and link budget, safety aspects...) that derived from the trajectory simulation and entry corridor design (where the bank angle profile is also optimized). This approach allows the definition of optimum and robust design solutions guaranteeing feasibility and margins coupling the AoA-Mach corridor (Flying Qualities) with the drag-velocity Entry Corridor (Trajectory Design).

In the Space Rider, a similar process was applied, and extended to the transonic and subsonic regimes, not covered by the IXV. Additionally, another degree of freedom was added to the problem, that is the variability of the aeroshape. At the beginning of the study, in phase A, a trade-off on the candidate aeroshape classes was carried out [3], resulting in the selection of the Lifting Body as baseline aeroshape class. Within the Lifting Body class, two options were analyzed: the IXV aeroshape, and the IXV aeroshape with fins (see Fig 5). On one side, the IXV aeroshape maximized the IXV heritage from any perspective and it ensured the extension of fly-ability envelope down to transonic and subsonic regimes.

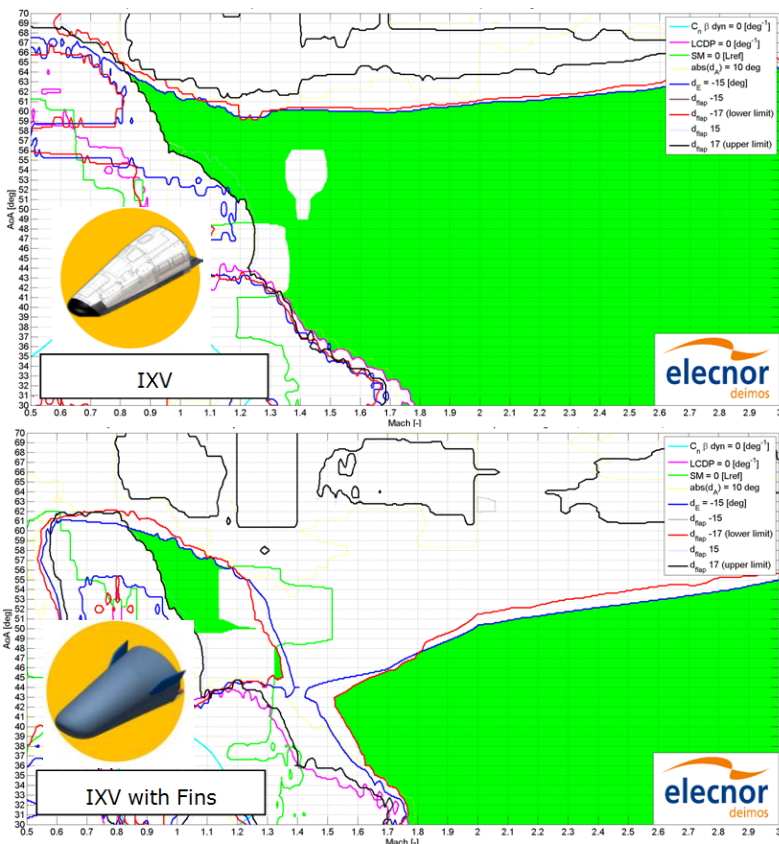


Fig 5. Supersonic to subsonic Angle of Attack corridor for the candidate Lifting body configurations

On the other, the IXV with fins was a promising variant especially in terms of maximization of the vehicle flight capability, and lateral-directional static and dynamic stability, even if with significant drawbacks in terms of mass increase, structural modifications and an additional effort for the characterization of the aerodynamics and aerothermodynamics properties. In this context, Flying Qualities (FQs) analyses were carried out focusing on the supersonic, transonic and subsonic regimes, assuming the IXV CoG location, to support the trade between the two solutions. The comparison between the two configurations and the FQ results confirmed the possibility to cross the transonic/subsonic regimes with the IXV configuration (Fig 5 shows how the AoA Mach corridor closes at Mach ~1.6 for the IXV with fins configuration), that was the selected as the baseline solution for the Space Rider Preliminary design.

The software used to perform all the Flying Qualities analyses is the DEIMOS Space S.L.U. FQA Analysis Tool that has also been extensively used in multiple projects of the European Space Agency [4]. More details and results of both FQs and trajectory design are presented in the next sections.

4. Flying Qualities

The vehicle configuration design (the aeroshape definition, CoG location and trim line design solution) is provided as an input for the Mission and GNC design disciplines. Flying Qualities (FQ) are evaluated with dedicated Monte Carlo functionalities of the FQA Tool in order to characterize the trim, stability, and control characteristics, and margins as input to GNC activities. For the baseline configuration selected, a trim line design solution was identified within the available entry corridor (Fig 6). Because the AoA-Mach corridor narrows below Mach 1, and closes at approximately Mach 0.8, the DRS box (Mach 0.5-0.8) cannot be reached with the trim line solution, and an alternative trim strategy has been explored: when the flaps/elevators reached a maximum deflection, the elevon is frozen and the vehicle is allowed to "free fly" (i.e. AoA is let free for trim with the aileron and the sideslip angle). This solution is valid from a FQ perspective if the aileron is not saturated as well and it basically leverage on the high pitch stability of the vehicle in transonic/subsonic. The drawback of the "free flight" approach is a wider variability in the AoA that is obtained against a closed loop control strategy, that have an impact on the trajectory (a dispersion in AoA leads to a dispersion in L/D and therefore on the range controllability during free flight) and on the Descent sub-system (a wide dispersion on AoA could become a challenging requirement for the drogue parachute design).

Results presented in this section are based on a Monte Carlo campaign of 4000 shots including uncertainties on aerodynamics, AoA tracking, inertia properties, dynamic pressure, CoG location and GNC allocation in all flight regimes. The evaluated FQs comprise trim characteristics, static and dynamic stability, dynamic couplings, spin tendency, and hinge moment needs. Fig 8 shows, for example, the 99% range of variability (blue: lower limit; red: upper limit) with 90% confidence level for the trim elevon deflection, sideslip angle and the dynamic $C_{n\dot{\beta}}$. The dynamic $C_{n\dot{\beta}}$ is defined as a function of the roll and yaw torque coefficients derivative with respect to the sideslip angle, and is both a static stability and a Dutch-roll stability indicator. Levels of $C_{n\dot{\beta}}$ above $1E-3 \text{ deg}^{-1}$ are considered satisfactory. The results of the campaign verify and validate that an optimal and robust solution has been designed for the current configuration achieving good overall performances with margins. The AoA corridor is verified and good performances are validated down to Mach 0.9, with no saturations on the control surfaces, acceptable sideslip variability and no relevant dynamic instabilities. Below Mach 0.9, the "free flight" trim strategy is considered applicable, with similar performance to the classic (IXV) trim line approach in terms of stability and controllability. The "free flight" approach was thus selected as the baseline trim solution at the end of phase B1, for the given configuration.

The supersonic, transonic and subsonic FQs have been validated afterwards with the results of the 6 DoF GNC Monte Carlo for the Entry and TAEM phase [7], in particular the trim performance. The variability from the FQ results properly predicts the variability obtained with the GNC (Fig 7 shows for example the aileron deflection), and the margins assumed in the FQ analyses are appropriate.

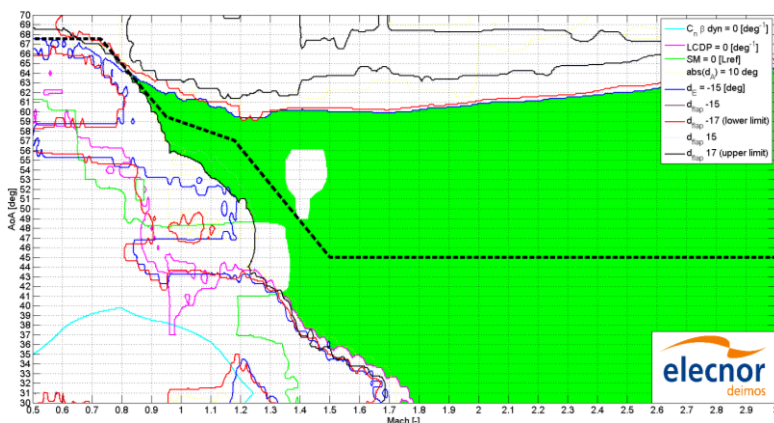


Fig 6. Trimline solution for Space Rider

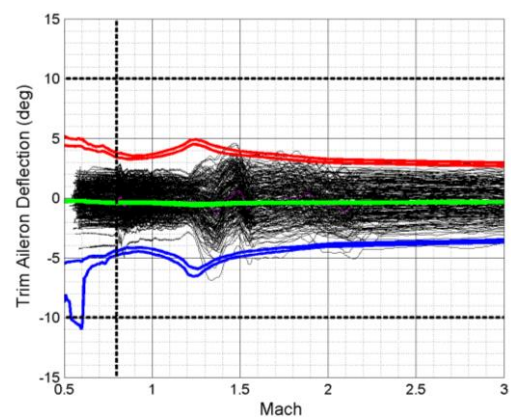


Fig 7. Validation of FQ prediction with 6DoF GNC results

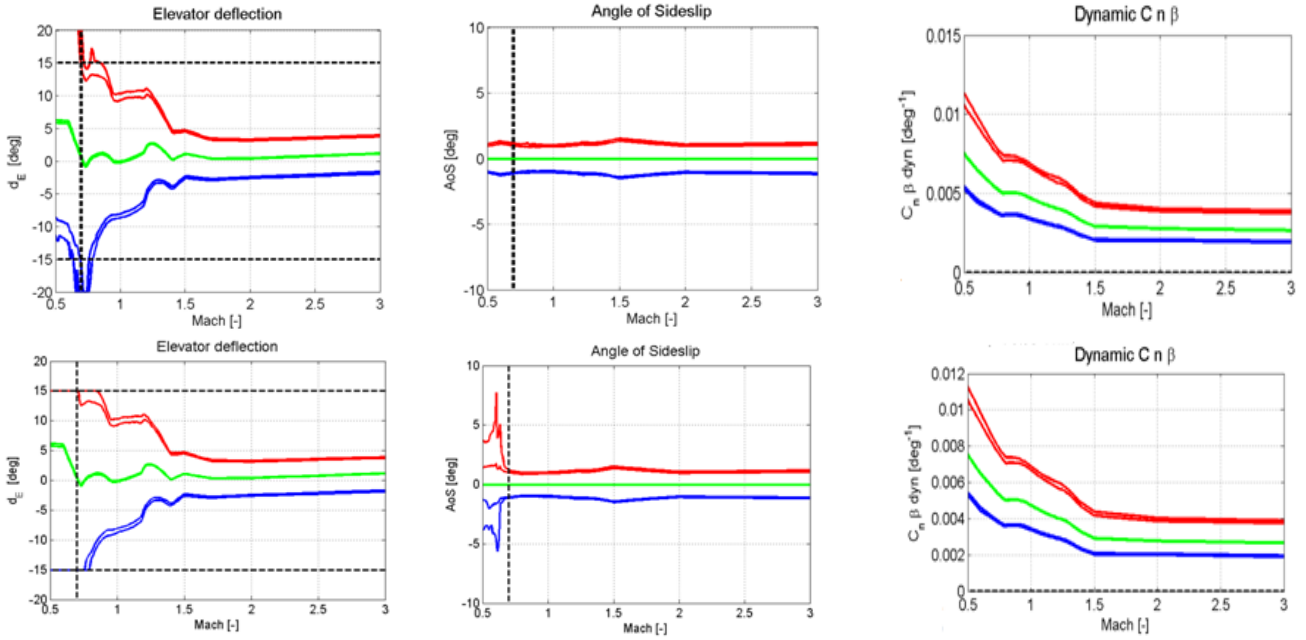


Fig 8. Elevon deflection, AoS, and dynamic $C_{n\beta}$ variability, fixed trim line (up) vs free flight trim strategy (down)

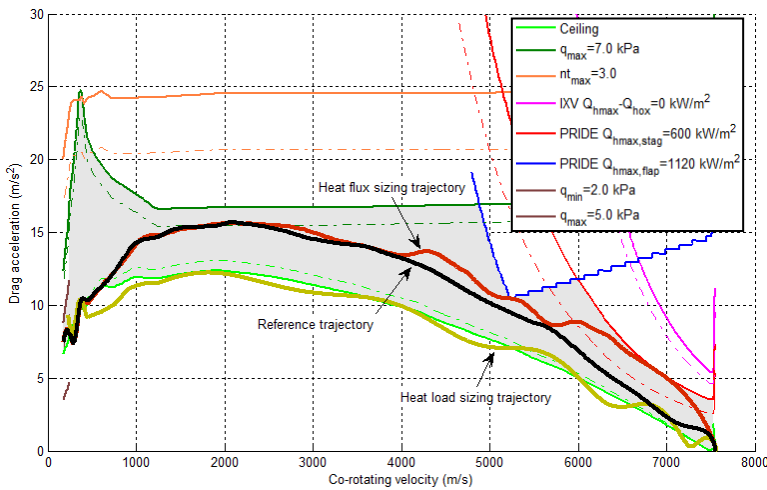


Fig 9. Reference and sizing trajectories w.r.t. Entry Corridor

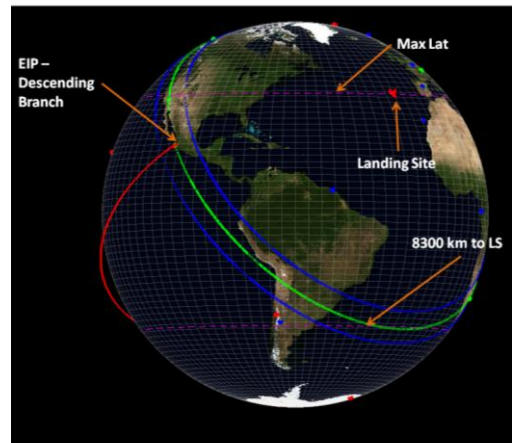


Fig 10. EIP targeting for Azores

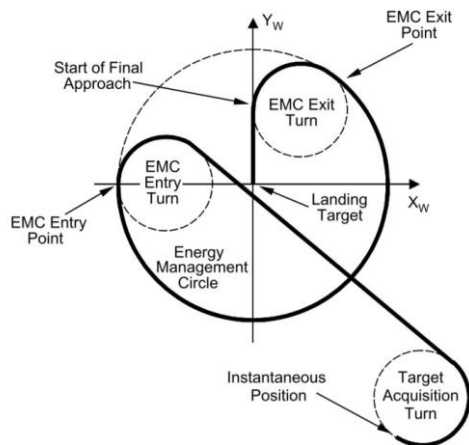


Fig 11. Reference Parafoil Guidance strategy of the X-38 mission

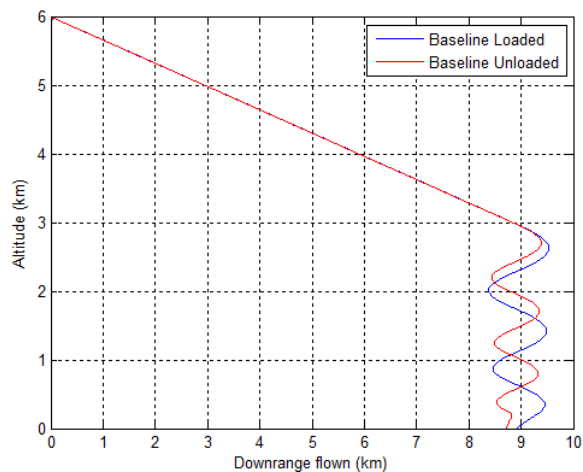


Fig 12. Parafoil flight for different SR RM configurations

5. End-to-End Trajectory Design

The trajectory design is a multiphase problem where the definition of the reference mission needs to be compatible with all of the Mission and System constraints with adequate margins for GNC operation. The considered constraints include the deorbit opportunities from the operative orbit to the desired landing site within the landing site network, vehicle thermo-mechanical limits during entry, stability and controllability through the trim line design during hypersonic/supersonic/ transonic and subsonic regimes, DRS activation limits and descent system operative envelopes, safety restrictions to Entry Interface Point (failure footprint), mass margin policy, and visibility from ground stations.

For a given scenario and vehicle configuration, the entry corridor is defined as the flight domain where the vehicle can fly being compliant with the imposed constraints (Fig 9), whose limits are defined by a combination of technology capability (the technology behind each subsystem defines the design limits), System limitations (it can be decided at System level to limit a subsystem below its capabilities in order to avoid oversizing of the vehicle) and mission boundaries (a ceiling limit is designed to ensure no skip-out and return into orbit in case of shallow returns) and are never to be exceeded. Within the Entry Corridor, the sizing trajectories are trajectories that activate the constraint that defines the corridor, and are used for the design of a particular system/subsystem that activates a particular constraint. For the Space Rider, sizing trajectories for the heat flux and heat load were computed to support the design of the Thermal Protection System (see Fig 9), for the maximum mass configuration.

Once the Entry Corridor is defined, the reference trajectory is computed. The computation of the reference trajectory requires a single end to end optimization process from deorbiting to the triggering of the Descent and Recovery System (DRS). The objective of the optimized deorbiting and coasting maneuver is to target the desired conditions (position, velocity and attitude) at the beginning of the entry phase (at the Entry Interface Point, EIP). These conditions have to be compatible with the Entry Corridor limits and with the range capability to reach the desired landing site (see Fig 10). The objective of the entry phase optimization is to calculate an optimum reference trajectory from the EIP to the targeted DRS conditions, compliant with all the entry constraints and assuring maximum margins for the GNC during the entry of the vehicle. The entry optimization is a Full Optimal Control Problem that involves several parameters and control profiles. The software used is based on the DEIMOS Space S.L.U. Sequential Gradient Restoration Algorithm (SGRA) [5]. The SGRA is an indirect full optimal control algorithm that allows the optimization of a control profile along with a determined set of parameters having an effect on the problem under study. Specifically, the optimization code developed for IXV [2] was adapted for the Space Rider.

Feasible and optimum end-to-end trajectories were computed for the baseline and backup scenarios (see Fig 13), providing margins for the GNC operations within the entry corridor and being compatible with the orbital phases, the descent system operative envelope and the targeted landing sites. The higher velocity at the EIP when deorbiting from a 37 deg orbit with respect to an equatorial orbit (7530 m/s versus 7430 m/s), coupled with a higher mass with respect to IXV (~2550 kg) forced to target a shallower entry than for IXV (-1.17 deg vs -1.21 deg). Thermal constrains, at the vehicle nose and at the flaps, including passive to active oxidation limit for C-SiC Thermal Protection System (TPS) material and transition to turbulence, are respected.

For the return from a medium inclination orbit, a preliminary analysis concluded that 1-2 opportunities exist to reach the same landing site within 24 h, with other solutions available also for alternative landing sites such as Kourou, the Canary Islands, or Ascension. From a quasi equatorial orbit, even more deorbit opportunities are expected.

Preliminary trajectory solutions were computed for the descent under parafoil phase. For this phase of the flight, the trajectory geometry definition depends strongly on the guidance strategy implemented, and the glide performance vary with respect to the parafoil aerodynamic capability, wind loading, and atmospheric density. The wind profile has also a profound impact on the trajectory, because the wind velocity may be comparable to the glide velocity. In order to guarantee enough margin for trajectory control, the maneuvering energy should be preserved as long as possible. For a constant glide flight, the maneuvering energy corresponds to altitude. A solution similar to the X-38 strategy [6] was assumed (see Fig 11), and preliminary trajectories were computed for different vehicle configurations (see Fig 12).

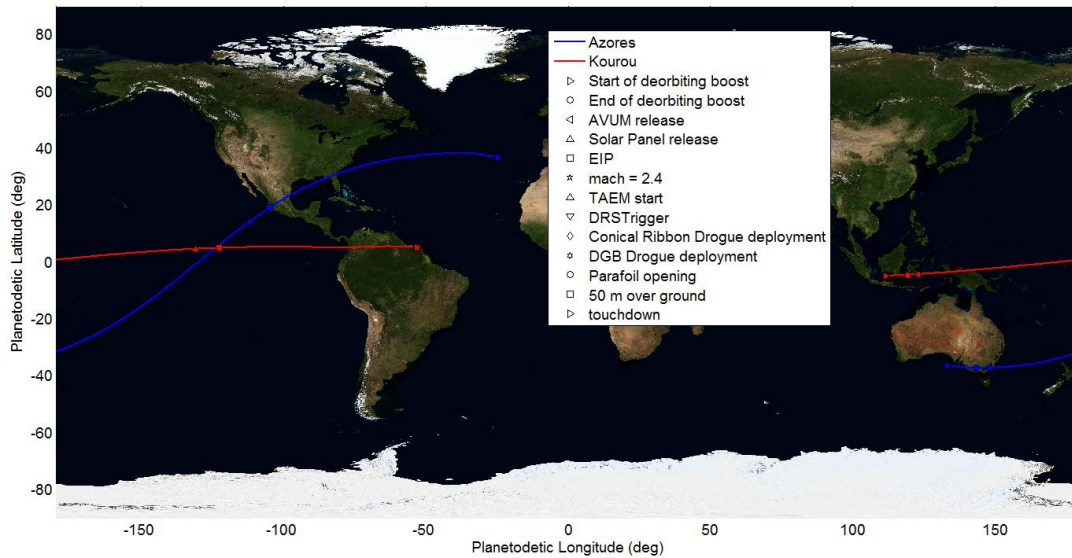


Fig 13. Baseline and backup reference trajectories groundtrack

6. Mission Performance

The performance and robustness of the mission were preliminarily validated using a full simulation from deorbiting to parafoil deployment in the baseline mission scenario. An end-to-end Monte Carlo campaigns of 1000 shots has been simulated. It comprises the de-orbiting maneuver, ballistic orbital arc until AOM-RM separation, the coasting of the RM until the Entry Interface Point, the guided entry and TAEM phase, and the descent under the pilot, subsonic conical ribbon and Disk-Gap-Band parachutes. These simulations included a proto-Guidance in close loop derived from the Entry and TAEM phases Space Rider Guidance [7], and Navigation and Control performance models inherited from IXV [2][8]. Simulations have been conducted considering uncertainties in the AVUM AOCs pointing accuracy during the deorbiting maneuver, environment, and vehicle characteristics (mass properties, aerodynamics).

The dispersions at the EIP strongly depend on the accuracy of the deorbit maneuver, and are in general aligned to the dispersions considered for the IXV qualification (see Fig 14). During entry, the constraints are fulfilled, in particular ATD, with the exception of the heat flux at flap in worst case conditions that presents a minor violation (see Fig 17). Anyhow, both the definition of the worst case conditions and the ATD model are currently under revision in the phase B2, in particular with the experience gathered during the IXV flight, where lower than predicted heat fluxes were recorded.

The entry proto-Guidance is able to compensate the large dispersions at the EIP and achieve performance at approximately Mach 1.6 comparable to the IXV, and mainly driven by the Navigation error (see Fig 18). The TAEM proto-Guidance controls the trajectory during the supersonic and transonic phase further reducing the position dispersion (see Fig 19), and targets the desired heading dispersion to guarantee a precise alignment of the trajectory toward the reference DRS conditions. The pilot triggering is estimated to occur within the DRS box and the in the descent phase the system flies mainly within the parachutes operative envelopes (Fig 16). Performance are indicating that iterations at system levels are necessary to converge to a Descent design compatible with specifications that can be derived from these analyses. This is considered as normal work in next design loops. Position accuracy at the targeted parafoil deployment at approximately 6 km of altitude is lower than 9 km, well within the capabilities of the current parafoil solution ($L/D \sim 3$).

The mission performance predicted by Mission Analysis have been compared with the results of the 6 DoF GNC Monte Carlo for the Entry and TAEM phase [7], in order to validate the MA design process, assumptions, and results against simulations with actual Guidance, Navigation, and Control functions in the loop. The GNC results are in line with the predictions obtained in Mission Analysis, demonstrating the validity of the trajectory analysis process and assumptions. In particular, the position dispersion with the proposed Entry and TAE solution for Space Rider considerably improves with respect to the error induced by the IXV Navigation (see Fig 18 and Fig 19).

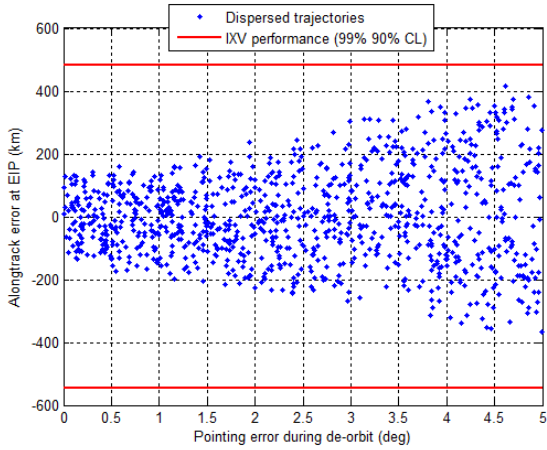


Fig 14. Alongtrack error at EIP

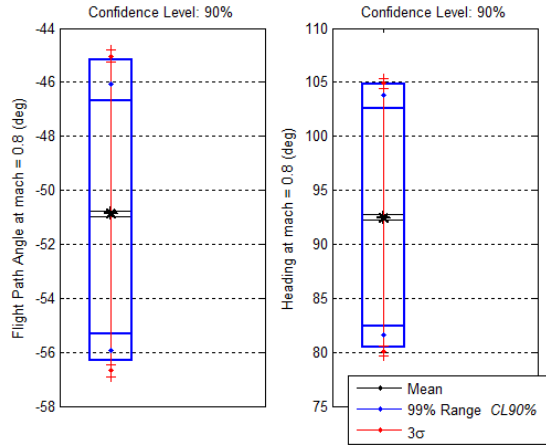


Fig 15. FPA and heading variability at DRS

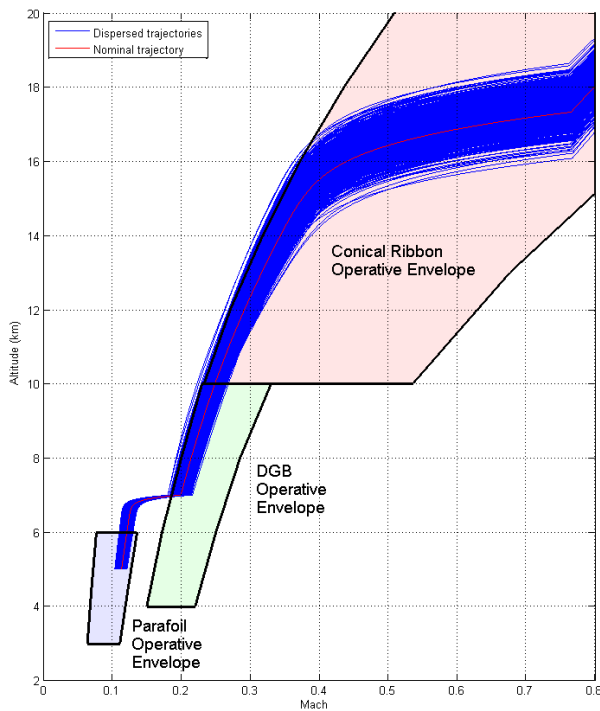


Fig 16. Dispersed descent trajectories

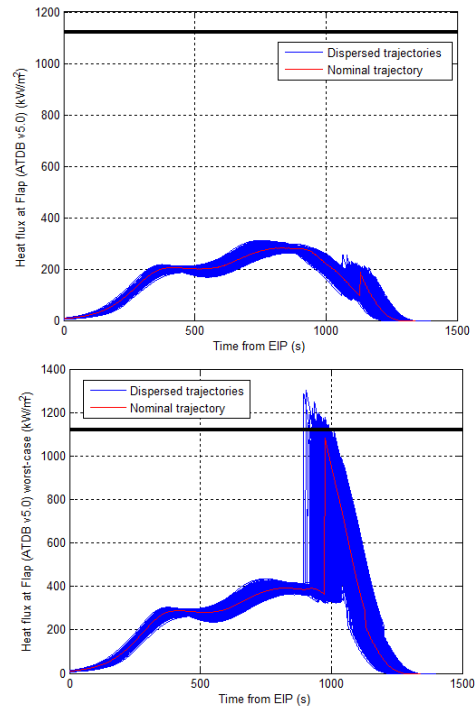


Fig 17. Heat flux at flap performance

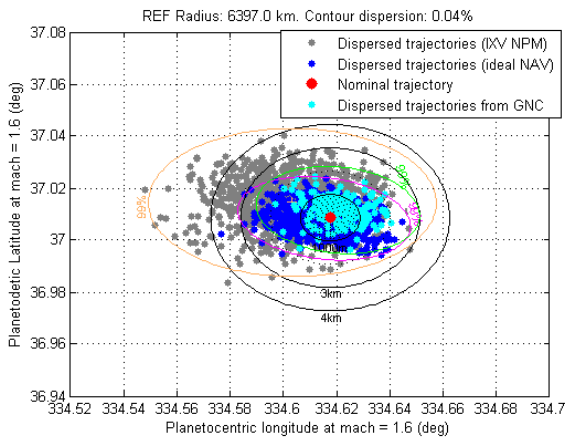


Fig 18. Position dispersion at end of Entry

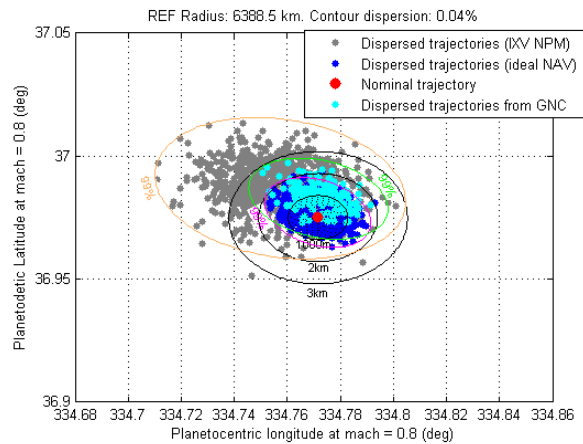


Fig 19. Position dispersion at targeted DRS

7. Safety Analyses

In addition to the footprint for the nominal scenario, the corresponding non-nominal footprint in case of a failure of the Space Rider has been preliminary derived by combining the results of the IXV safety footprint [2] with the Space Rider range capability, in line with the phase A/B1 safety/risks assessment needs. For the IXV, the failure case analyzed was a complete GNC loss occurring in any moment of the flight between the separation from the AVUM and the DRS triggering. A Monte Carlo campaign of more than 140.000 shots was run based on free 6-DoF propagation of the IXV with the failure (initial condition) occurring at any moment of any of the nominal scenario Monte Carlo trajectories. Advanced statistical methods for low probability events estimation has been applied to estimate stable 10^{-5} and 10^{-7} boundaries.

The analysis was carried out for the baseline scenario of a return from a 37 deg orbit to land at Santa Maria, Azores, considering the Gridded Population of the World Model v4.0 (GPW4 [9]), extrapolated to the targeted date of the mission (2020). The estimated footprint is shown in Fig 20.

The total casualty probability on ground for a return to Azores is estimated to be $1.56E-06$, with over 93% of the casualty risk contributed by the Azores islands themselves, despite their low population. If the probability that this event occurs is set to 1% (as per Space Shuttle Orbiter [10]), the casualty is estimated to be $1.56E-08$, compatible with the safety requirements. It is mentioned that if Kourou is considered as a target landing site, the projected footprint is going to cover higher land area percentage, eventually resulting into higher risk than for the Azores landing scenario. Dedicated safety analyses involving all the landing solutions are being executed within phase B2 of the programme.

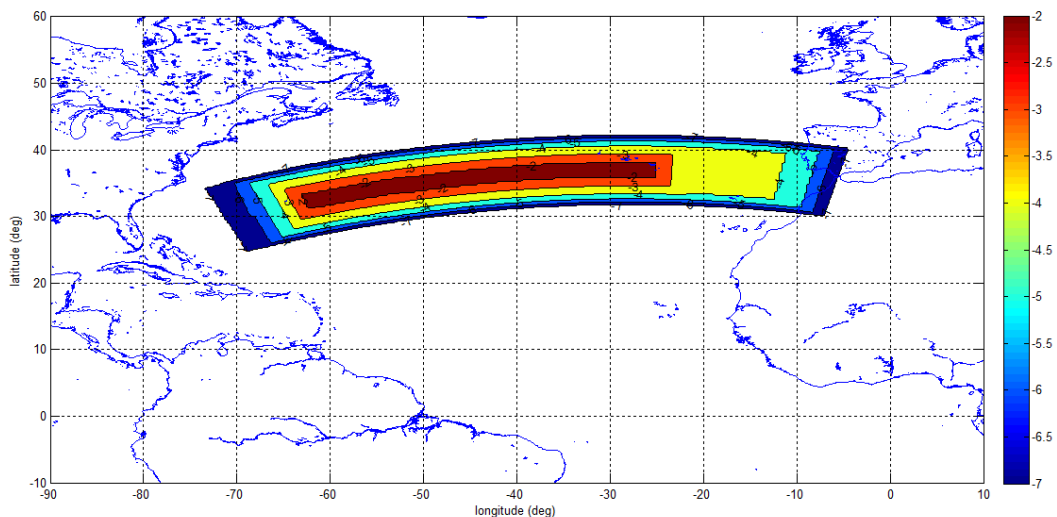


Fig 20. Estimated footprint for AZORES landing site

8. Visibility Analyses

The first objective of the visibility analysis is to evaluate the existence of a line of sight between the Space Rider and a given station of the Ground Station Network (GSN) considering the station antenna mask and SR antennae pattern, in order to evaluate the capability to download to the network of ground stations the telemetry, and with the objective of maximize visibility during the critical events of the mission.

A preliminary geometric visibility analysis has been performed for the end-to-end baseline and backup missions from deorbiting to landing, considering the preliminary baseline GSN solution (Core ESA network, Cooperative network, Augmented network, see Fig 21) and different ground stations masks (elevation $> 5^\circ$ or elevation $> 0^\circ$). About 14000 km of downrange are flown during the deorbiting (~ 1000 km) and coasting (~ 13000 km) phases in about 33.5 minutes. Additional 8300 km are flown during the entry. Following the Space Rider, with continuous visibility from ground stations, results to be extremely challenging. For the cases analyzed, a large part of the Space Rider trajectory is above the Pacific Ocean where few ground stations exist (South Point is the main one). Fig 21 shows the

complete set of ground stations and the ground track for the Azores and Kourou missions. Additionally, preliminary visibility analysis for the orbital phase are reported (red line) considering a 52 deg target orbit. For the baseline mission, deorbiting, coasting and descent phases are partially visible from Canberra and Santa Maria, respectively. Some short visibility is also possible from New Norcia, Perth and Dongara (much worse than from Canberra but maybe useful in the seconds right before deorbiting start). For the Kourou landing site, the descent phase is partially visible from Kourou, while the deorbiting and coasting visibility is not guaranteed. If larger fractions of coverage are needed, satellite data relay or movable stations in strategic points could be considered. A consolidation of the visibility analysis is expected in next phases with a consolidated mission design.

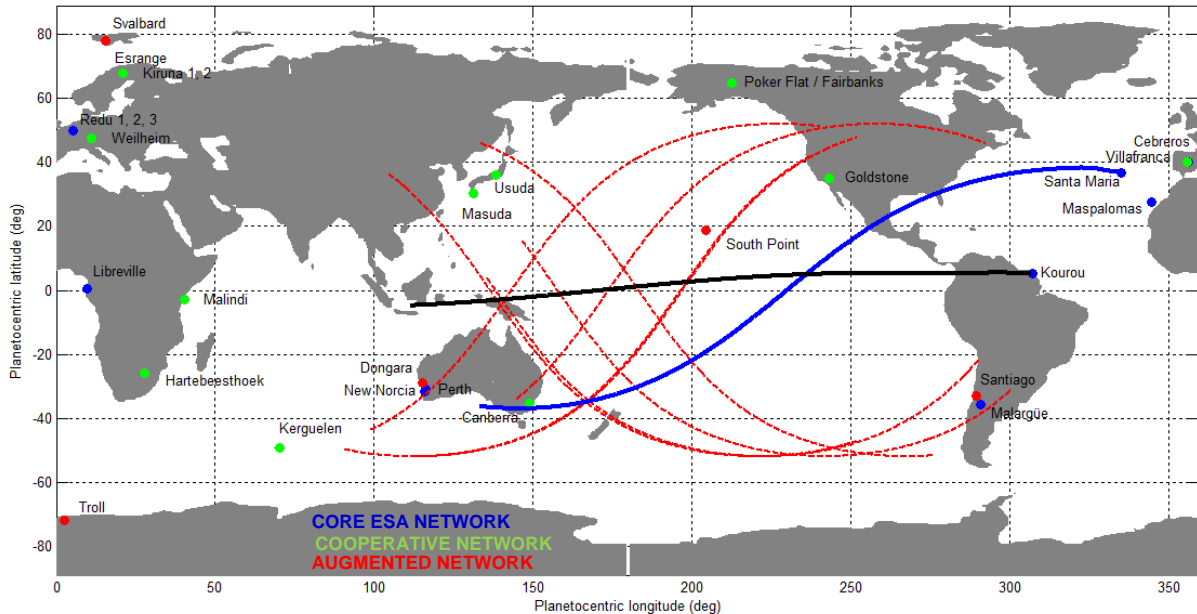


Fig 21. Ground station network and Space Rider E2E ground track. Blue = Azores; Black = Kourou (Red = preliminary results for orbital phase)

9. Conclusions

During the phase A/B1 of the Space Rider Mission Analysis, multiple activities have been performed to support the trade-offs at system level for the definition of the baseline vehicle configuration and mission solution. The baseline solution feasibility has been assessed, including high fidelity simulations and optimizations of the complete return phase (from deorbiting to touchdown), leveraging on consolidated tools and DEIMOS Space Mission Analysis expertise inherited from the IXV mission. Driving factors that should be tackled in the next phases of the programme have been identified: consolidation of the system mass budget, further characterization of the aerodynamic properties in supersonic and subsonic, review of the ATD model according to IXV flight performance, consolidation of the descent system design, full definition of the ground station network, and specification of the safety requirements and limitation especially close to the targeted landing sites.

Considerable variability exists between the different Space Rider mission scenarios in terms of orbit, conditions at the EIP (FPA, velocity), range to be flown during entry and landing sites. These imply the need for a significant missionization process of the Space Rider programme.

Continuous iterations with System activities are currently ongoing as part of the Mission Analysis activities for the phase B2 of Space Rider, with the overall objective of consolidating the current baseline toward a successful System Preliminary Design Review, and to derive specifications for the design of the Space Rider subsystems.

Acknowledgments

The work has been performed under the Space Rider programme in Phase A/B1 and funded by the European Space Agency. The authors wish to thank SENER, Thales Alenia Space Italia, CIRA and ESA teams, for their support to the Space Rider mission analysis activities in Phase A/B1.

References

1. Tumino G. et al (2013) "The PRIDE Programme: From The IXV To The ISV", IAC-13, Cape Town, South Africa.
2. Bonetti D. et al. (2015) "IXV Mission Analysis And Flight Mechanics: From Design To Postflight", 23rd AIDAA, Turin, Italy.
3. Marini M. et al (2017) "Aeroshape Trade-Off and Aerodynamic Analysis of the Space Rider Vehicle", 7th EUCASS Conference, Milan, Italy.
4. Haya R. et al (2011) "Flying Qualities Analysis for Re-entry Vehicles: Methodology and Application", AIAA GNC 2011, Portland, USA.
5. Bastante J.C. et al (2010) "End to end Optimisation of IXV Trajectory via Multiple-Subarc Sequential Gradient Restoration Algorithm", 61st IAC, Prague, Czech Republic.
6. Stein J. et al (2005) "An Overview of the Guided Parafoil System Derived from X-38 Experience ", 18th AIAA Aerodynamic Decelerator Systems Technology Conference, Munich, Germany.
7. De Zaiacomo G. et al (2018) "SPACE RIDER: Entry and TAEM GNC of the Future European Reusable Space Transportation System", HiSSt Conference, Moscow, Russia.
8. Marcos V. et al (2016), "The IXV Guidance, Navigation and Control Subsystem: Development, Verification and Performances", Acta Astronautica, Vol. 124.
9. Gridded Population of the World (GPW) v4.0 (2015), Socioeconomic Data and Applications Center (SEDAC), <http://www.ciesin.org/>
10. Hamlin T.L. et al (2010) "2009 Space Shuttle Probabilistic Risk Assessment Overview", 10th International Probabilistic Safety Assessment and Management Conference, Seattle, USA.